DOI: 10.1002/ejoc.200500978

Towards an Understanding of the Polar Diels–Alder Reactions of Nitrosoalkenes with Enamines: A Theoretical Study

Luis R. Domingo,*[a] M. Teresa Picher,[a] and Pau Arroyo[a]

Keywords: Diels–Alder reactions / Nitrosoethylenes / Reaction mechanisms / Electrophilicity / Density functional calculations

The polar Diels–Alder reactions of nitrosoalkenes with enamines have been studied using DFT methods at the B3LYP/6-31G* level of theory. These Diels–Alder reactions are characterized by a nucleophilic attack of the enamine at the conjugated position of the nitrosoalkene with concomitant ring-closure. The reactions present a total regioselectivity and a large *endo* selectivity. The analysis, based on the global electrophilicity of the reagents in the ground state, the natural bond orbital (NBO), and the topological analysis of the electron localization function (ELF) in the *endo* transition state (TS) and "halfway" along the IRC between the TS and cycloadduct, correctly explain the polar nature of these cycloaddition reactions. The large electrophilic character of nitrosoethylenes together with the large nucleophilic character of enamines are responsible for the large acceleration found in these polar Diels–Alder reactions.

Introduction

Organocatalysis has received much attention in organic chemistry because of the obvious advantages over metal-mediated catalysis; it does not need expensive and often toxic metals, and the organocatalysts are generally easier to make and more easily recoverable than standard catalytic reagents.[1] The most utilized strategy in organocatalysis is one that generates nucleophilic enamines from any number of aldehydes or ketones followed by direct bond-forming reactions with a wide variety of electrophiles.[2] Further, since these catalysts can also generate imines during their reactions, electrophilic catalysts might facilitate diverse reactions with nucleophiles. Secondary amines such as pyrrolidine (**1**)[3] and chiral L-proline[4] have been used as organocatalytic molecules that accelerate a range of transformations such as aldol,[5] Mannich,[6] Michael,[7] and Diels–Alder (DA)[3,8] reactions.

Oxazine derivatives have been widely used in organic synthesis because they can be readily converted into a wide variety of derivatives such as oxazinones, pyrrolidines, pyrroles, amino alcohols, amines, 1,3-dicarbonyl compounds, and other interesting products.[9] Oxazines **4** have been obtained from the DA reaction between nitrosoethylenes **3**, which act as heterodienes, and olefinic substrates such as enol ether, enamines, alkenes or allenes (see Scheme 1). Oxazines have also been obtained from DA reactions between 1,3-dienes and nitroso compounds R–NO, which act as heterodienophiles.[10] The highly reactive nitrosoethylenes can be generated through base-mediated dehydrohalogenation of available α-halooximes **2** and furnish the cycloadducts **4** in a highly regioselective fashion.[11] The use of Lewis acid catalysts to increase the reactivity of nitrosoalkenes **3** is not feasible because they increase the high reactivity of these species leading to the formation of undesired dimerization products and polymers.[12] A mixture of aldehydes and catalytic amounts of secondary amines can reversibly generate strongly nucleophilic enamines that can participate in polar DA reactions with electrophilic reagents. Recently, Jorgensen and co-workers[13] reported the first catalyzed DA reaction of nitrosoalkenes generated in situ from α-halooximes using pyrrolidine as the organocatalyst (see Scheme 2). These DA reactions involve enamine intermediates (**9**) formed by condensation of the carbonyl compounds **6** with pyrrolidine **1**. Subsequent hydrolysis of the amine acetals **10** releases the final hydroxyoxazines, **7** (Scheme 3). Nitrosoalkenes bearing electron-releasing (ER) substituents such as **14** were less reactive than those bearing electron-withdrawing (EW) groups. Thus, the 4-nitrophenyl- and the ethoxycarbonyl-nitrosoalkenes **12** and **11** were highly reactive (see Scheme 4).[13]

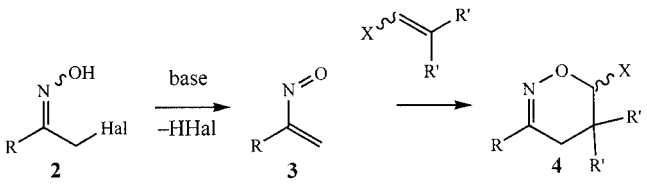

Scheme 1.

[a] Instituto de Ciencia Molecular (UIQOT), Departamento de Química Orgánica, Universidad de Valencia, Polígono "La Coma", 46980 Paterna, Valencia, Spain

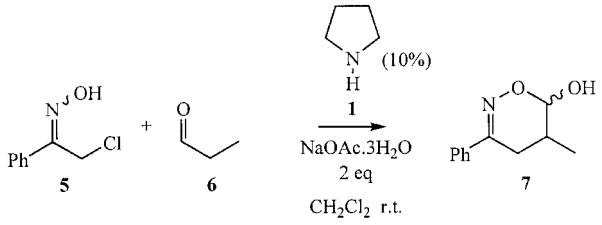

Scheme 2.

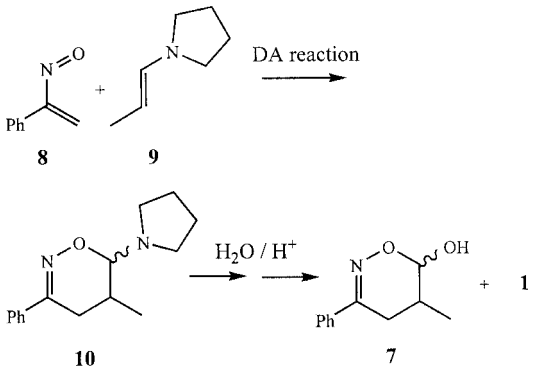

Scheme 3.

Several theoretical reports have appeared describing the use of nitroalkenes in DA reactions. Density functional theory (DFT) studies on the molecular mechanism of the DA reactions of nitroethylenes with electron-rich ethylenes (methyl vinyl ether and dimethylvinylamine) have shown that these reactions are highly asynchronous concerted processes which can formally be viewed as being induced by nucleophilic attack of the electron-rich ethylene at the conjugated position of nitroethylene which acts as the electrophilic center.[14] The feasibility of this reaction has been related to the polar character of the transition-state (TS) structure;[14a] for instance, while for dimethylvinylamine, the more nucleophilic species of the series, the cycloaddition presents a very low activation energy, the reaction with methyl vinyl ether requires the presence of a Lewis acid coordinated to nitroalkene to make it feasible.[15]

The use of the global electrophilicity index ω,[16] defined within DFT,[17] has been reported to classify the dienes and dienophiles currently used in DA reactions on a unique scale of electrophilicity.[18] A good correlation between the difference in electrophilicity of the diene and dienophile pair, $\Delta\omega$, and the feasibility of the cycloaddition was found. For instance, the nitroethylene/methyl vinyl ether and nitroethylene/dimethylvinylamine cycloaddition reactions, which have been classified as polar cycloadditions, present a $\Delta\omega$ of 2.19 and 2.34 eV, respectively, while the butadiene/ethylene cycloaddition reaction, which is the prototype of a pericyclic cycloaddition, presents a $\Delta\omega$ of 0.41 eV. For the nitroethylene series, the higher value of $\Delta\omega$ for the stronger nucleophilic character of the substituted ethylene is in agreement with the lower activation energy.

Our interest in organocatalysis[19] prompted us to carry out a theoretical investigation of the DA reaction involved in the pyrrolidine-catalyzed reaction of nitrosoalkenes studied recently by Jorgensen and co-workers.[13] Two DA reactions have been studied. The first one is the DA reaction between the simplest nitrosoethylene **13** and the enamine **15** (see Scheme 6). For this reaction, both the regio- and stereoselectivities were considered. The second reaction is the DA reaction between the α-phenyl-nitrosoethylene **8** and the enamine **9**, a model reaction for those experimentally studied by Jorgensen and co-workers (see Scheme 8). The analysis of the global reactivity indexes in the ground state (GS) of the reagents, together with the natural bond orbital (NBO) and the topological analysis of the electron localization function (ELF), will be used to explain the polar nature and the large acceleration found in these DA reactions.

Results and Discussion

First, a DFT analysis based on the global reactivity indexes of the reactants involved in these DA reactions will be performed. Then the energetic aspects and the geometrical parameters of the TSs and their electronic structures in terms of bond orders, natural charges, and ELF analysis of these polar DA reactions will be analyzed. The energetic results including solvent effects, modeled as a continuum model, will be also discussed.

DFT Analysis Based on the Reactivity Indexes

Recent studies devoted to DA reactions[18,20] have shown that the global indexes defined in the context of DFT are a powerful tool with which to understand the behavior of polar cycloaddition reactions. The static global properties, electronic chemical potential μ, chemical hardness η, and global electrophilicity ω, of a series of nitrosoethylenes **8**, **11**–**14** and enamines **9** and **15** are presented in Table 1.

Table 1. Electronic chemical potential (μ), chemical hardness (η), and global electrophilicity (ω) of nitrosoethylenes **8**, **11**–**14** and enamines **9** and **15** (see Scheme 4).

	μ [au]	η [au]	ω [eV]
11	–0.1872	0.1151	4.14
12	–0.1843	0.1181	3.91
13	–0.1675	0.1158	3.30
8	–0.1654	0.1191	3.12
14	–0.1584	0.1140	3.00
Nitroethylene	–0.1958	0.2002	2.60
Methyl vinyl ether	–0.0895	0.2564	0.42
15	–0.0590	0.2315	0.20
9	–0.0554	0.2284	0.18

The electronic chemical potential of the enamines **9** and **15**, μ = –0.0554 and –0.0590 au, respectively, are lower than those of the nitrosoethylenes **8**, **11**–**14**, μ ranges from –0.1872 to –0.1584 au, thereby indicating that alongside a polar cycloaddition reaction, net charge transfer (CT) will take place from the enamines towards the nitrosoethylenes, in clear agreement with the CT analysis performed on the corresponding TS (see later).

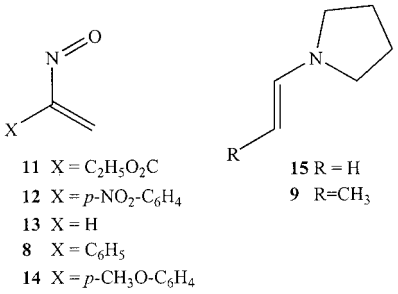

Scheme 4.

The electrophilicity of the simplest nitrosoethylene **13** is 3.30 eV, a value that falls in the range of strong electrophiles within the ω scale.[18] This value is larger than that of nitroethylene (ω = 2.60 eV).[18] Although the nitrogen atom of nitroethylene supports a partial positive charge, see the Lewis structures **A** and **B** in Scheme 5, delocalization of the formal negative charge of the oxygen atoms onto the NO_2 framework can be responsible for the smaller electrophilic character of nitroethylene compared with nitrosoethylene.

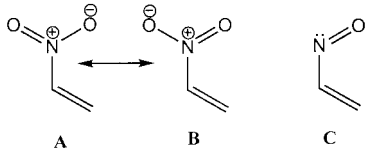

Scheme 5.

The presence of a phenyl substituent at the α position of nitrosoethylene reduces the electrophilicity of **8** to 3.12 eV. The large electrophilic character of the nitrosoethylene framework causes the phenyl group present in **8** to behave as an ER group. The electrophilicity of α-phenylnitrosoethylenes is modified by substitution of the phenyl substituent. Thus, inclusion of an ER CH_3O group at the *para* position of the phenyl group lowers the electrophilicity of **14** to 3.00 eV, while the inclusion of a strong EW NO_2 group in **12** raises it to 3.91 eV. Substitution of the α position of nitrosoethylene by a strong EW carboxy group increases the electrophilicity of the nitrosoethylene **11** to 4.14 eV.

On the other hand, the vinylamines **9** and **15** have very low electrophilicity values, 0.18 and 0.20 eV, respectively. These vinylamines are classified as marginal electrophiles (good nucleophiles).[20a] The presence of an ER methyl substituent on the enamine **9** lowers the electrophilicity compared with **15**. These low electrophilicity values, which are lower than that of methyl vinyl ether (ω = 0.42 eV),[18] indicate that these enamines will participate as strong nucleophiles in polar cycloaddition reactions.[14a]

A good correlation has been found between the difference in the electrophilicity of the reagent pair, $\Delta\omega$, and the CT in the corresponding TS.[18] Consequently, $\Delta\omega$ has been used as a measure of the polar character of cycloaddition reactions. The value of $\Delta\omega$ for the reaction between nitrosoethylene **13** and vinylamine **15** is high, 3.10 eV, indicating that the corresponding cycloaddition reaction will have a large polar character. Note that this value, which is higher than that for the nitroethylene/dimethylvinylamine cycloaddition, 2.34 eV, is a consequence of the strong electrophilic character of the nitrosoethylene and the strong nucleophilic character of the enamine.[20a]

Exploration of the Potential Energy Surface for the Polar DA Reactions between Nitrosoethylenes and Enamines

Two computational models have been chosen to study these cycloaddition reactions. The first one, Model I, corresponds to the DA reaction between the simplest nitrosoethylene (**13**) and 1-vinylpyrrolidine (**15**) (see Scheme 6). The regioselectivity, the formation of *ortho* and *meta* cycloadducts, and the stereoselectivity, the *endo* and *exo* approach modes of 1-vinylpyrrolidine to nitrosoethylene, of this reaction were studied. In Model II, the reaction between (1-nitrosovinyl)benzene (**8**) and 1-[(*E*)-prop-1-enyl]pyrrolidine (**9**) studied experimentally by Jorgensen and co-workers[13] is considered (see Scheme 8).

The Polar DA Reaction between Nitrosoethylene (13) and 1-Vinylpyrrolidine (15)

Owing to the asymmetry of both the heterodiene and the ethylene derivative, four reactive channels are feasible for this cycloaddition. These are related to the formation of the *ortho* and *meta* regioisomeric cycloadducts and the *endo* and *exo* approach modes of 1-vinylpyrrolidine to nitrosoethylene. For Model I, all four reactive channels were studied. An exhaustive exploration of the potential energy surface (PES) associated with these cycloaddition reactions led to the discovery of only one TS corresponding to a highly asynchronous bond formation process. We also found a molecular complex (**MC1**) associated with a very early stage of the reaction and situated on a very flat region of the PES which controls the access to the different reactive channels. **MC1** is more stable than the isolated reactants **13** + **15** and the distance between the two fragments of the complex is around 2.5–2.9 Å. Note that these MCs subsist only on the gas-phase PES. However, their presence allows us to explain why some of the TSs are lower in energy than the reagents (see later). Therefore, one molecular complex (**MC1**) and four TSs (**TS1on**, **TS1ox**, **TS1mn**, and **TS1mx**; those associated with the *ortho* and *meta* channels are named as **o** and **m** and those with the *endo* and *exo* channels are named as **n** and **x**, respectively) were located and characterized (see Scheme 6). The *endo* and *exo* channels yield a pair of enantiomeric cycloadducts. Therefore, only two cycloadducts **16** and **17**, associated with the *ortho* and *meta* regioisomeric channels, respectively, were considered. The total and relative energies are summarized in Table 2. The geometries of the TSs are shown in Figure 1.

The relative electronic energies of the TSs associated with the four cycloaddition modes are –1.8 (**TS1on**), 0.3 (**TS1ox**), 10.0 (**TS1mn**), and 12.5 kcal/mol (**TS1mn**). The energy of **TS1on** is less than that of the reagents. However, if we consider the formation of the molecular complex **MC1**, the potential energy barrier becomes slightly positive; there is an inverted energy profile and the corresponding

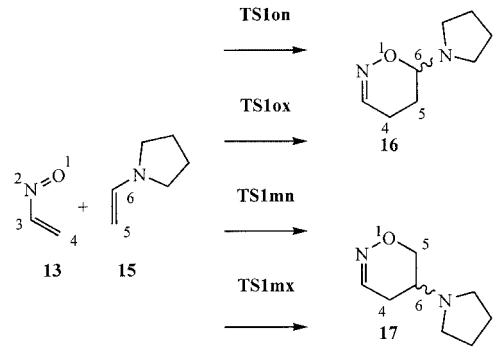

Scheme 6.

Table 2. Total (E) and relative[a] (ΔE) energies (E_{sol} and ΔE_{sol} are the energies in dichloromethane) of the stationary points of the Diels–Alder reactions between the nitrosoethylenes **8** and **13** and the vinylamines **9** and **15** calculated at the B3LYP/6-31G* level of theory.

	E [au]	ΔE [kcal/mol]	E_{sol} [au]	ΔE_{sol} [kcal/mol]
MC1	–497.862799	–3.2	–497.865502	0.5
TS1on	–497.860471	–1.8	–497.867231	–0.6
TS1ox	–497.857187	0.3	–497.864425	1.2
TS1mn	–497.841686	10.0	–497.849082	10.8
TS1mx	–497.837795	12.5	–497.846554	12.4
16	–497.929884	–45.3	–497.935637	–43.5
17	–497.922313	–40.6	–497.928057	–38.8
MC2	–768.238487	–2.5	–768.241733	1.5
TS2n	–768.238386	–2.4	–768.244541	–0.3
TS2x	–768.232850	1.1	–768.240179	2.5
TS3	–768.225395	5.7	–768.239504	2.9
ZW	–768.231976	1.6	–768.255260	–7.0
10a	–768.310756	–47.8	–768.316228	–45.3
10b	–768.303543	–43.3	–768.309019	–40.7

[a] Relative to **13** and **15** or **8** and **9**.

value of the potential energy barrier is 1.4 kcal/mol. Note that this barrier is less than that computed for the DA reaction between nitroethylene and dimethylvinylamine at the same level of theory (8.3 kcal/mol)[14a] as a consequence of the stronger electrophilic character of the nitrosoethylene **13** compared with nitroethylene. This reaction presents complete *ortho* regioselectivity as **TSmn** is 11.8 kcal/mol higher in energy than **TS1on**, in clear agreement with the results of experiments; only amine acetals such as **7** are observed.[13] The stereoselectivity, measured as the energy difference between the *endo* and the *exo ortho* TSs, is 2.1 kcal/mol. The formation of the oxazines **16** and **17** is strongly exothermic, between –45.3 and –40.6 kcal/mol. Therefore, these cycloaddition reactions can be considered as irreversible. The strong electrophilic character of the nitrosoethylene **13** and the large nucleophilic character of 1-vinylpyrrolidine **15** are responsible for the low electronic activation barriers.

Several theoretical studies on related DA reactions have indicated that the activation energies calculated at the MP3/6-31G*[21] and B3LYP/6-31G*[22] levels of theory are in quite reasonable agreement with activation energy values determined experimentally. In view of the very low activation energy found for the DA reaction between **13** and **15**, single-point energy calculations at the MP3[23] and CCSD(T)[24] computational levels were performed on the B3LYP/6-31G*-calculated geometries in order to validate the DFT results. The total and relative energies obtained at these computational levels are given in Table 3. Both computational methods calculate **MC1** to have an energy of around 4 kcal/mol less than that of the reagents, in agreement with the DFT results. However, while the activation barrier for the cycloaddition reaction, relative to **MC1**, is 8.9 kcal/mol by the MP3 calculations, this decreases to 5.2 kcal/mol by the CCSD(T) ones. Although these values are 7.5 and 3.8 kcal/mol higher than those obtained at the B3LYP level, they indicate a large acceleration of this polar DA reaction. Finally, according to both these computational methods the process is around 10 kcal/mol more exothermic than the DFT results suggest; in all cases the process can be considered irreversible.

Table 3. Total (E) and relative[a] (ΔE) energies of the stationary points of the Diels–Alder reaction between nitrosoethylene **13** and 1-vinylpyrrolidine **15** calculated at the MP3/6-31G* and CCSD(T)/6-31G* level of theory.

	MP3/6-31G*		CCSD(T)/6-31G*	
	E [au]	ΔE [kcal/mol]	E [au]	ΔE [kcal/mol]
MC1	–496.2920771	–4.0	–496.380401	–4.2
TS1on	–496.2779861	4.9	–496.372057	1.0
16	–496.3720878	–54.2	–496.454745	–50.9

[a] Relative to **13** and **15**.

The geometries of the TSs are shown in Figure 1. Along the *ortho* reactive channels the length of the C4–C5 forming-bond in the TSs is 2.278 Å for **TS1on** and 2.263 Å for **TS1ox**, while the distance between the O1 and the C6 atoms is 2.913 Å for **TS1on** and 2.778 Å for **TS1ox**. Theses large distances indicate that these atoms are not being bonded. Along the *meta* reactive channels the length of the forming C4–C6 bond in the TSs is 1.814 Å for **TS1mn** and 1.880 Å for **TS1mx**, while the distance between the O1 and the C5 atoms is 2.624 Å for **TS1mn** and 2.558 Å for **TS1mx**. The extent of the asynchronicity can be measured from the difference between the distances of the bonds that are being formed in the reaction, that is, $\Delta r_{ortho} = d$(O1–C6) – d(C4–C5) and $\Delta r_{meta} = d$(O1–C5) – d(C4–C6). For the TSs, the Δr values are 0.63 (**TS1on**), 0.51 (**TS1ox**), 0.67 (**TS1mn**), and 0.47 (**TS1mx**). Thus, the *endo* TSs are more asynchronous than the *exo* ones. The C3–C4–C5–C6 dihedral angles of the *ortho* TSs are 43.9° (**TS1on**) and 65.9° (**TS1ox**). These values indicate that these TSs correspond to the *gauche* approach of the C3–C4 and C5–C6 double bonds along the C4–C5 bond formation. The larger deviation of the dihedral angle in **TS1on** is a consequence of the favorable coulombic interactions at this *endo* zwitterionic TS (see later), which close the dihedral angle.

Analysis of the atomic motions at the unique imaginary frequency of the more favorable *ortho* TSs, 239.2i cm^{-1} (**TS1on**) and 258.8i cm^{-1} (**TS1ox**), indicates that they are mainly associated with the movement of the C4 and C5 atoms along the C4–C5 bond-forming path, movement of the O1 and C6 atoms being negligible. This analysis rein-

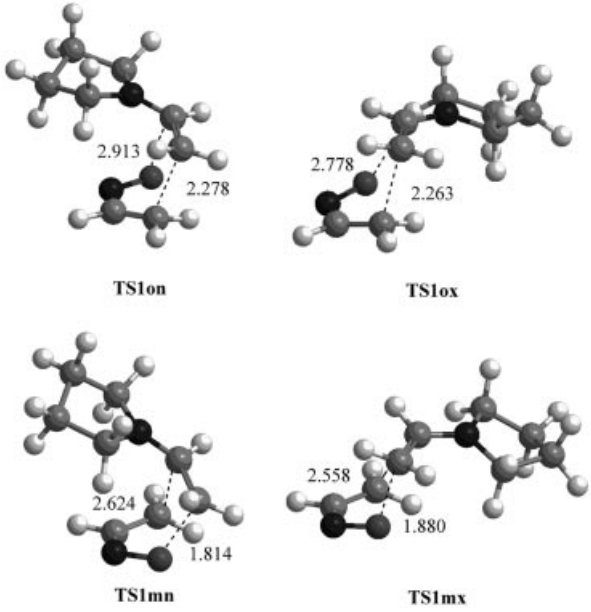

Figure 1. Geometries of the transition-state structures involved in the Diels–Alder reaction between nitrosoethylene **13** and 1-vinylpyrrolidine **15**. The distances are given in Å.

forces the two-center interaction of these polar cycloaddition reactions. Analysis of the atomic motions at the unique imaginary frequency of the *meta* TSs, 457.5i cm^{-1} (**TS1mn**) and 448.8i cm^{-1} (**TS1mx**), indicates that the O1–C5 and C4–C6 bond formations are coupled. The most favorable **TS1on** has the lowest imaginary frequency.

The intrinsic reaction coordinate (IRC) calculations on the more favorable *ortho* TSs show that these reaction channels directly connect the TSs with the cycloadduct **16** without the participation of any zwitterionic intermediate. Analysis of the points along the IRCs shows that these cycloaddition reactions are concerted two-stage processes.[25] In the first stage, the C4–C5 bond is completely formed in the nucleophilic attack of the C5 position of 1-vinylpyrrolidine on the C4 carbon atom of nitrosoethylene. The O1–C6 bond is formed in the second stage of the reaction. From the analysis of the IRC from **TS1on** to cycloadduct **16** we have selected the "halfway" point, **HFPon**,[26] which shares the reaction coordinates in the two stages. Note that **HFPon** is not a stationary point. The geometry of **HFPon** is shown in Figure 2. At this point in the reaction the length of the C4–C5 bond is 1.598 Å, while the distance between the O1 and C6 atoms remains 2.575 Å. The asynchronicity of the bond formation in **HFPon**, Δr_{ortho} = 0.98, is larger than that of the corresponding **TS1on**, 0.63.

The extent of bond formation along a reaction pathway is provided by the concept of bond order (BO).[27] The value of BO for the C4–C5 forming-bond in the *ortho* TSs is 0.33 for **TS1on** and 0.32 for **TS1ox**, while the value of BO between the O1 and the C6 atoms is 0.08 for **TS1on** and 0.06 for **TS1ox**. For the *meta* TSs, the BO value for the O1–C5 forming-bond is 0.52 for **TS1mn** and 0.48 for **TS1mx**, while the BO value between the C4 and C6 atoms is 0.29 for **TS1mn** and 0.24 for **TS1mx**. The *ortho* TSs form earlier in the reaction path and are more asynchronous than the *meta* ones. While the *ortho* TSs correspond to highly asynchronous bond formation processes, only the C4–C5 bond is being formed in the TS, the more energetic *meta* TSs correspond to asynchronous bond formation processes in which the O1–C5 bond formation is more advanced than the C4–C6 one. The BO value for C4–C5 in **HFPon**, 0.92, indicates that this bond has already formed, while the BO value between the O1 and C6 atoms is 0.22.

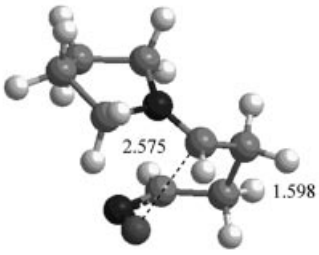

Figure 2. Geometry of the "halfway" point **HFPon** on the IRC between **TSon** and the [4+2] cycloadduct **16**. The bond lengths between the atoms directly involved in the reaction are given in Å.

The natural population analysis (NPA) allows the CT in these polar cycloaddition reactions to be evaluated. The B3LYP/6-31G*-calculated natural atomic charges in the TSs have been partitioned between the enamine and the nitrosoethylene frameworks. The negative charge transferred from the donor enamine to the acceptor nitrosoethylene is 0.32*e* for **TS1on**, 0.29*e* for **TS1ox**, 0.43*e* for **TS2mn**, and 0.39 *e* for **TS2mx**, thereby confirming the zwitterionic nature of these TSs. In these polar cycloaddition reactions there is large CT as a consequence of the strong electrophilicity of nitrosoethylene and the strong nucleophilic character of the enamine. The CT in the *endo* TSs is greater than that in the *exo* ones, whilst the CT in the *meta* TSs is greater than that in the *ortho* ones because the latter form earlier along the reaction path. However, CT increases to a maximum 0.61*e* for the **HFPon** formed along the *ortho* reactive channels.

Finally, the topologies of the ELF of nitrosoethylene **13**, enamine **15**, **TS1on**, the structure **HFPon**, and the cycloadduct **16** were analyzed in order to obtain additional information about the electron density evolution in these polar DA reactions. The population *N* of the valence basins of these structures are listed in Table 4. Nitrosoethylene **13** presents seven valence basins, namely V(O1), V(N2), two V(O1,N2), V(N2,C3), and two V(C3,C4). Whereas the two monosynaptic basins correspond to lone pairs on the O1 and N2 atoms, the disynaptic basins V(O1,N2) and V(C3,C4) correspond to the two double bonds represented in the Lewis structure of **13** in Scheme 7. The populations of the two monosynaptic basins are around 2.7*e*. On the other hand, the more significant valence basins of the enamine **15** are two monosynaptic basins on the N7 nitrogen, V(N7), with a total population of 2.41*e*, and three disynaptic basins, two V(C5,C6) with a population of 1.78*e* and 1.95*e* and one V(C6,N7) with a population of 1.95 *e*.

Table 4. The valence basin population *N* calculated for the ELF of the reagents, the TS, "halfway" on the IRC, and the cycloadduct involved in the more favorable *ortho*/*endo* pathway of the Diels–Alder reaction between nitrosoethylene **13** and 1-vinylpyrrolidine **15**.

Basin	Basin population *N* [*e*]			
	13 and **15**	**TS1on**	**HFPon**	**16**
V(O1)	2.64	2.87	2.88	2.57
V(O1)			3.07	2.47
V(O1,N2)	2.70	2.80	2.80	
V(O1,N2)	1.80	1.49	1.20	0.98
V(N2)	2.68	2.76		2.85
V(N2,C3)	2.01	2.26	3.26	3.23
V(C3,C4)	1.77	3.33	2.05	2.02
V(C3,C4)	1.71			
V(O1,C6)				1.27
V(C4,C5)			1.66	1.86
V(C5,C6)	1.78	3.29	2.17	1.99
V(C5,C6)	1.95			
V(C6,N7)	1.95	2.21	3.00	1.84
V(N7)	1.48	1.06	1.02	2.09
V(N7)	0.93	0.83		0.30

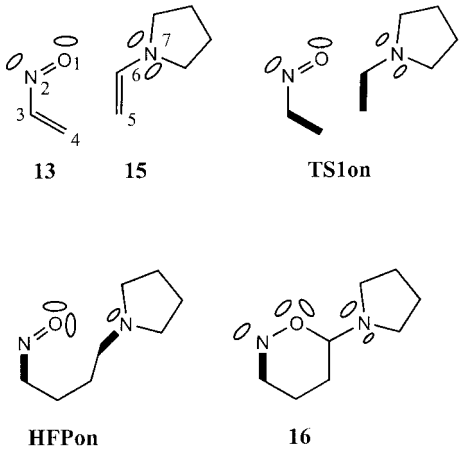

Scheme 7.

The more relevant changes found for the ELF of **TS1on** relative to those of the reagents are the fusion of the two disynaptic basins V(C3,C4) of **13** to a unique disynaptic basin V(C3,C4) with a population of 3.33*e* and the fusion of the two disynaptic basins V(C5,C6) of **15** to a unique disynaptic basin V(C5,C6) with a population of 3.39*e*. A flow of the electron population from the enamine fragment to the end of the nitrosoethylene fragment is observed in the TS. Thus, the total population of the monosynaptic basins on the N7 nitrogen decreases from 2.41*e* for the enamine **15** to 1.89*e* for **TS1on**, while the population of the disynaptic basin V(C6,N7) increases from 1.95*e* to 2.21*e*. On the other hand, a slight increase in the electron population of the nitrosoethylene fragment is observed; the sum of the population of the corresponding valence basins rises from 15.31*e* to 15.51*e*.

TS1on has no monosynaptic basins on the C4 and C5 carbon atoms. These will be created in a subsequent step of the IRC between the two atoms at a short distance and before the formation of the disynaptic basin V(C4,C5) associated with the formation of the C4–C5 bond.[42d]

The most interesting changes in the electron population along the IRC are observed for the **HFPon** structure for which the creation of the disynaptic basin V(C4,C5) with a population of 1.66*e* indicates C4–C5 bond formation. While the N7 nitrogen presents a unique monosynaptic basin with a population of 1.02*e*, the disynaptic basin V(C6,N7) increases to 3.00*e*. In addition, while the C5 carbon atom is sp^3-hybridized, the C6 remains sp^2. A new monosynaptic basin is created on the O1 atom which adds to the previous one to give a total population of 5.95*e*. Furthermore, the population of the disynaptic basin V(C3,C4) decreases to 2.05*e*, while the population of V(N2,C3) increases to 3.26*e*. These changes indicate a large polarization of the **HFPon** structure associated with the formation of the C4–C5 bond. Note that for **HFPon** there is no monosynaptic basin associated with the C6 carbon atom which is required before O1–C6 bond formation.

Finally, for the cycloadduct **16**, as well as the presence of a new disynaptic basin V(O1,C6), remarkably N7 again has two monosynaptic basins with a total population of 2.39*e*. As a consequence, the lone pair on the N7 nitrogen of the enamine **15** has a large incidence in this polar cycloaddition reaction, it being responsible for the strong nucleophilic character of **15**.

The amount of CT in this polar process has been evaluated from the sum of the core and valence basins of the enamine and nitrosoethylene fragments in **TS1on** and **HFPon**. The CT from the enamine **15** to the nitrosoethylene **13** is 0.31*e* in **TS1on** and 0.67*e* in **HFPon**. This large CT found in the C4–C5 bond formation, which is closer to that obtained by NPA analysis, shows the polar nature of these highly asynchronous concerted cycloaddition reactions, as anticipated by the electrophilicity analysis of the reagents.

The solvent effects of dichloromethane were modeled using the PCM method by means of single-point calculations on the gas-phase-optimized geometries. The relative energies are reported in Table 2. Solvent effects stabilize all stationary points by between 2 and 6 kcal/mol. Owing to their zwitterionic character, the more stabilized species are the nitrosoethylene **13** and the TSs associated with the nucleophilic attacks. As a consequence, in dichloromethane, the energy of **MC1** is located 0.5 kcal/mol above the reagents, while **TS1on** is located 0.6 kcal/mol below. **TS1on** remains 11.4 kcal/mol below **TS1mn**. The *exo* TSs are more stabilized than the *endo* ones, however, **TS1on** remains 1.8 kcal/mol below **TS1ox**, the cycloaddition reaction being *endo* selective.

The Polar DA Reaction between (1-Nitrosovinyl)benzene (8) and 1-[(E)-Prop-1-enyl]pyrrolidine (9)

Four reactive channels are also feasible for the cycloaddition reaction between (1-nitrosovinyl)benzene (**8**) and 1-[(*E*)-prop-1-enyl]pyrrolidine (**9**). However, owing to the complete regioselectivity shown by the cycloaddition reaction Model I, only the *endo* and *exo* approach modes along the *ortho* regioisomeric channels were considered (see

Scheme 8). An exhaustive exploration of the PES along each one of the two stereoisomeric reactive channels allowed us to find again only one TS associated with a highly asynchronous bond formation process. Therefore, one molecular complex **MC2**, two TSs (**TS2n** and **TS2x** associated with the *endo* and *exo* channels and denoted as **n** and **x**, respectively), and their corresponding cycloadducts **10a** and **10b** were located and characterized (see Scheme 8). The total and relative energies are summarized in Table 2. The geometries of the TSs are given in Figure 3.

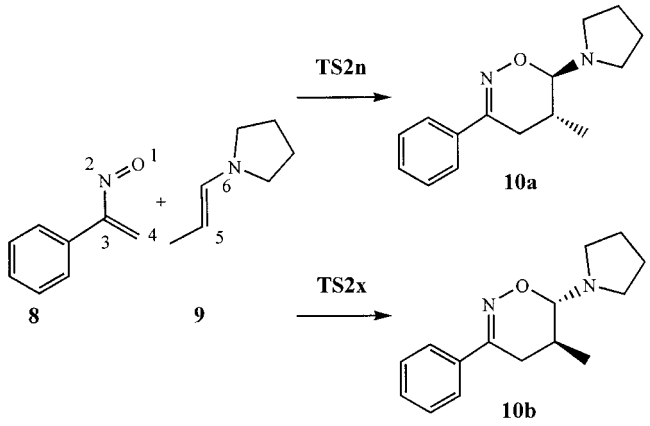

Scheme 8.

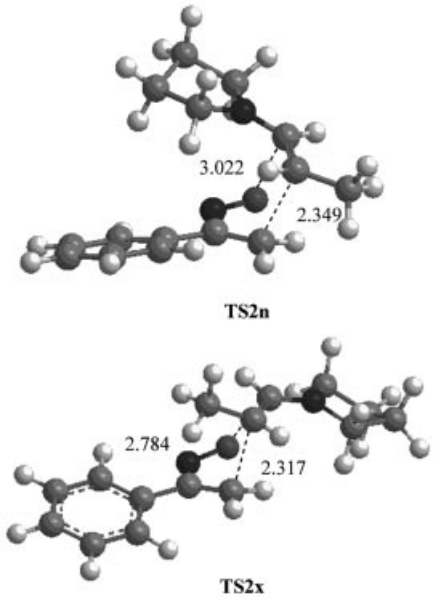

Figure 3. Geometries of the *endo* and *exo* transition-state structures involved in the Diels–Alder reaction between nitrosoethylene **8** and vinylpyrrolidine **9**. The distances are given in Å.

These cycloaddition reactions are highly asynchronous bond formation processes associated with a Michael-type addition of the enamine **9** to the conjugated position of the nitrosoethylene **8**. The relative electronic energies of the TSs associated with these nucleophilic attacks are –2.4 (**TS2n**) and 1.1 kcal/mol (**TS2x**). The value of the relative energy of the most favorable **TS2n** with respect to the separate reagents is negative; however, if we consider the formation of **MC2**, the potential energy barrier becomes slightly positive, 0.1 kcal/mol. The strong electrophilic character of the nitrosoethylene **8** and the strong nucleophilic character of the enamine **9** are both responsible for the very low electronic activation barriers associated with C–C bond formation in this reaction. This cycloaddition reaction presents a large *endo* stereoselectivity, **TS2n** is 3.5 kcal/mol lower in energy than **TS2x**. The formation of the oxazines is strongly exothermic, –47.8 (**10a**) and –43.3 kcal/mol (**10b**); oxazines **10a** and **10b** are a pair of enantiomers but with different conformations. Therefore, the cycloaddition step of these organocatalytic reactions can be considered as irreversible. After the formation of the amino acetals, acidic hydrolysis affords the corresponding hydro-oxazines (see Scheme 4).[13]

Owing to the fact that these cycloadditions are two-center addition reactions, a stepwise mechanism associated with the *anti* attack of the enamine **9** on the nitrosoethylene **8** can coexist.[14a] Therefore, the *anti* pathway was also studied (see Scheme 9).[28] The energetic results are summarized in Table 2 while the geometries of *anti* **TS3** and the corresponding zwitterionic intermediate **ZW** are shown in Figure 4. The potential energy barrier for **TS3** relative to **MC2** is 8.2 kcal/mol; the formation of the zwitterionic intermediate **ZW** is endothermic by 1.6 kcal/mol. *anti* **TS3** is located 8.1 kcal/mol above *endo* **TS2n**; consequently, in the gas phase the stepwise channel associated with the *anti* attack of the enamine **9** on the nitrosoethylene **8** is not competitive.[14a] The subsequent ring-closure of the intermediate **ZW** is nearly barrierless; both the C4–C5 bond rotation and the O1–C6 bond formation have insignificant barriers.

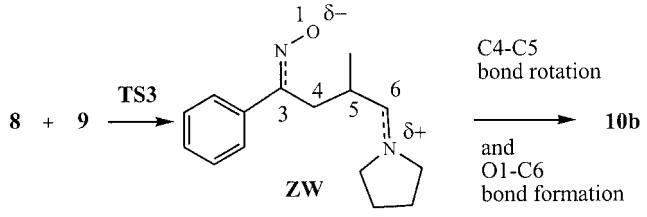

Scheme 9.

The geometries of the TSs and the zwitterionic intermediate are shown in Figure 3 and Figure 4. The length of the C4–C5 forming-bond in **TS2n** and **TS2x** is 2.349 and 2.317 Å, respectively, while the distance between the O1 and the C6 atoms is 3.022 and 2.784 Å, respectively. The O1–C6 distances indicate that these atoms are not being bonded. For the concerted TSs, the extent of the asynchronicity, that is, $\Delta r = d(\mathrm{O1–C6}) - d(\mathrm{C4–C5})$, is 0.67 for **TS2n** and 0.47 for **TS2x**. The more favorable *endo* TS is more asynchronous than the *exo* one. For *anti* **TS3** the length of the C4–C5 forming-bond is 2.052 Å, while it is 1.626 Å in the intermediate **ZW**, indicating that this bond has already formed. The C3–C4–C5–C6 dihedral angles for the TSs are 46.7 (**TS2n**), 77.2 (**TS2x**) and 163.8° (**TS3**). While **TS2n** and **TS2x** correspond to a *gauche* approach of the C3–C4 and C5–C6 double bonds along the C4–C5 bond formation reaction coordinate, **TS3** corresponds to the *anti* approach.

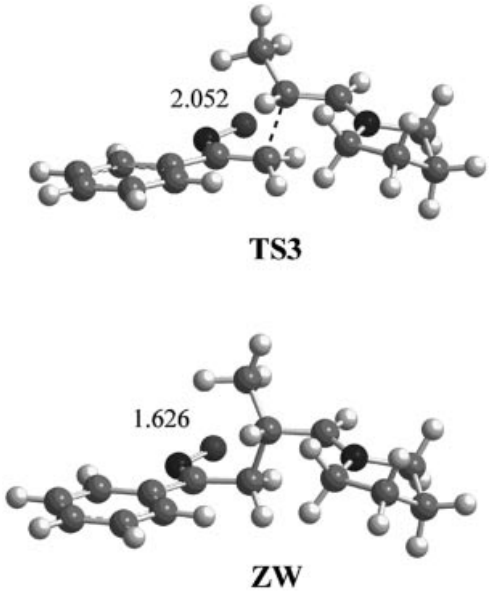

Figure 4. Geometries of the transition-state structure **TS3** and the zwitterionic intermediate **ZW** involved in the *anti* addition of the vinylpyrrolidine **9** to the nitrosoethylene **8**. The distances are given in Å.

The BO value for the C4–C5 forming-bond for the concerted TSs is 0.30 for **TS2n** and 0.20 for **TS2x**, while the BO value between the O1 and C6 atoms is 0.07 for **TS2n** and 0.04 for **TS2xn**. These BO values indicate the highly asynchronous character of the TSs. The *endo* TS is more advanced than the *exo* one. The BO value of the C4–C5 forming-bond in *anti* **TS3** is 0.46, while for the intermediate **ZW** it is 0.86. The more favorable concerted TSs are formed earlier than the *anti* **TS3**.

In this polar cycloaddition reaction, the negative CT that fluxes from the donor enamine to the acceptor nitrosoethylene is 0.32*e* for **TS2n**, 0.31*e* for **TS2x**, and 0.38*e* for **TS3** thereby confirming the zwitterionic nature of these TSs. In the zwitterionic intermediate **ZW** the CT is 0.57*e*. Note that this value is closer to that calculated for **HFPon**. Therefore, in these polar cycloaddition reactions the CT increases during the nucleophilic attack until completion of C–C bond formation. This large CT is a consequence of the strong electrophilicity of nitrosoethylene and the strong nucleophilic character of the enamine.

Analysis of the atomic motions at the unique imaginary frequency of concerted TSs, 187.4i (**TS2n**) and 227.6i cm^{-1} (**TS2x**), indicates that mainly movement of the C4 and C5 atoms occurs along the C4–C5 bond-forming path, movement of the O1 and C6 atoms being negligible. This analysis reinforces the two-center interaction of this polar DA reaction. While in the proline-catalyzed aldol reaction, formation of a hydrogen bond catalyzed the aldol addition very efficiently, also favoring the formation of the corresponding zwitterionic aminol intermediate,[19a] in the pyrrolidine-catalyzed DA reaction, the coulombic attraction between the ends of the zwitterionic TSs favor concomitant ring-closure to give the corresponding amino acetal in a concerted process.[14a]

Solvent effects stabilize all stationary points by between 2 and 15 kcal/mol. The more stabilized species are the nitrosoethylene **8**, the TSs, and the intermediate **ZW** as a result of their zwitterionic character. Now, in dichloromethane, **MC2** is located 1.5 kcal/mol above the reagents, while **TS2n** is located 0.3 kcal/mol below them. Also, the *exo* **TS2x** is more stabilized than the *endo* **TS2n**, in clear agreement with the large dipole moment of the former (4.26 D for **TS2n** and 5.47 D for **TS2x**). However, **TS2n** remains 2.8 kcal/mol below **TS2x**, the cycloaddition reaction being *endo* selective. The TS and intermediate associated with the *anti* attack are strongly stabilized, 8.9 (**TS3**) and 14.6 kcal/mol (**ZW**), as a consequence of their large zwitterionic character. In spite of this large stabilization, **TS3** remains 3.2 kcal/mol above **TS2n**, the concerted mechanism being more favorable than the stepwise one. However, for DA reactions involving more electrophilic nitrosoethylenes that can evolve a larger CT, such as the 4-nitrophenyl- and the ethoxycarbonyl-nitrosoalkenes **12** and **11**, the *anti* attack could be competitive.

Conclusions

The transition-state structures associated with the polar Diels–Alder reaction of nitrosoalkenes with enamines have been studied using DFT methods at the B3LYP/6-31G* level of theory. Analysis of the two σ bonds formed in these polar cycloaddition reactions indicates that they are highly asynchronous concerted processes involving nucleophilic attack of the enamine at the conjugated position of the nitrosoalkene, a Michael-type addition. Concomitant ring-closure with the formation of the C–O bond in the second stage of these concerted processes affords the corresponding oxazine. These reactions present a total *ortho* regioselectivity as a consequence of the more favorable two-center interaction in the conjugate addition to nitrosoethylene and a large *endo* selectivity as a consequence of favorable coulombic interactions between the ends of the zwitterionic *endo* TSs. The stepwise pathway associated with the *anti* attack of the enamine on the nitrosoethylene has also been characterized. In the model studied, the greater stabilization of the TS associated with *gauche endo* attack relative to that associated with the *anti* one makes the *anti* attack uncompetitive. However, for Diels–Alder reactions involving more electrophilic nitrosoethylenes, the *anti* attack could be competitive in the condensed phase as a consequence of the greater solvation of the corresponding zwitterionic *anti* TS. In these cases, the stronger electrophilic character of the nitrosoethylene derivative, together with the polarity of the solvent, can modify the reaction mechanism from a concerted to a stepwise one.

The analysis based on the global electrophilicity of the reagents correctly explains the polar nature of these cycloaddition reactions. The strong electrophilic character of nitrosoethylenes and the strong nucleophilic character of the enamines are responsible for the large acceleration found in these polar Diels–Alder reactions. The strong nu-

cleophile–electrophile interaction along the *ortho* reactive channels is responsible for the large regioselectivity found in these polar cycloaddition reactions.

Analysis of the ELF at selected points on the IRC shows that the concerted cycloaddition reactions are two-stage processes with C–C bond formation taking place in the first stage with O–C bond formation occurring at the end of the reaction. ELF analysis of the flow of the electron population in the cycloaddition reaction reinforces the results of our NBO analysis. In the cycloaddition reaction there is large charge transfer from the nucleophilic enamine to the strongly electrophilic nitrosoethylene leading to complete formation of the C–C bond.

Computational Methods

In recent years, theoretical methods based on DFT have emerged as an alternative to traditional ab initio methods in the study of the structure and reactivity of chemical systems. Cycloaddition reactions have been the subject of several DFT studies and have shown that functionals that include gradient corrections and hybrid functionals that allow for exchange and correlation effects, such as B3LYP,[29] together with the standard 6-31G* basis set,[23] lead to potential energy barriers that are in good agreement with experimental results.[30] So, in this study, geometrical optimizations of the stationary points were carried out using this methodology. The optimizations were carried out using the Berny analytical gradient optimization method.[31] The stationary points were characterized by frequency calculations in order to verify that the TSs have one and only one imaginary frequency. The IRC[32] path was traced in order to check the energy profiles connecting each TS to the two associated minima of the proposed mechanism by using the second-order González–Schlegel integration method.[33] The electronic structures of the stationary points were analyzed by the NBO method.[34] All calculations were carried out using the Gaussian 98 suite of programs.[35]

The solvent effects of dichloromethane, modeled as a continuum model, were determined by performing B3LYP/6-31G* single-point calculations on the gas-phase-optimized geometries using a relatively simple self-consistent reaction field (SCRF)[36] based on the polarizable continuum model (PCM) of Tomasi and co-workers.[37] The electronic energies in solution were obtained by adding the total electrostatic energies obtained from the PCM calculations to the electronic energies determined in vacuo. The PCM and solvent (dichloromethane) options were employed in the SCRF calculations.

The global electrophilicity index ω,[16] which is a measure of the stabilization energy when a system acquires additional electronic charge ΔN from the environment, is given by $\omega = (\mu^2/2\eta)$,[16] where μ is the electronic chemical potential and η the chemical hardness. Both quantities may be expressed in terms of the one electron energies of the HOMO and LUMO frontier molecular orbitals, ε_H and ε_L, that is, $\mu \approx (\varepsilon_H + \varepsilon_L)/2$ and $\eta \approx (\varepsilon_L - \varepsilon_H)$, respectively.[38]

The methods based on the topological analysis of the electron density or its Laplacian, such as the atoms-in-molecules (AIM) method of Bader[39] or the ELF approach of Becke and Edgecombe[40] and extensively developed by Savin and co-workers,[41] are suitable for the visualization of the electronic redistribution along a reaction pathway. Several topological analyses have recently been undertaken to gain a better understanding of bonding and chemical reactivity.[42]

The ELF has been defined as a measure of the local Pauli repulsion and its topological analysis provides us with a useful and convenient partitioning of molecular space into regions that are associated with chemically meaningful concepts such as atomic shells, bonds, and lone pairs. Each region, called a basin, is related to a local maximum (i.e., an attractor) of the ELF and it is interpreted as a region in which localization of an electron or a pair of electrons is more probable. The basins are either core basins labeled C(A) or valence basins labeled V(A,…) belonging to the outermost shell. Valence basins are characterized by their coordination number (the synaptic order) to the core. Hence, lone pairs are represented by monosynaptic basins, while covalent bonding between two atoms by disynaptic basins. A quantitative analysis is performed through the integration of the electronic density $\rho(\boldsymbol{r})$ in the volume of the ELF basin Ω. The integrated basin population (N_i) of a given basin is calculated using Equation (1).

$$N_i = \int_{\Omega_i} \rho(\mathrm{r}) d\mathrm{r} \tag{1}$$

Following N_i along a calculated reaction path is a useful technique that allows the specific flow of electronic charge in a chemical reaction to be identified as well as a rational characterization of chemical concepts such as bond-forming and -breaking processes, providing new insights on the reaction mechanism. ELF analysis was carried out using a cubical grid with a step size of less than 0.1 bohr employing the TopMod[43] package of programs.

Acknowledgments

P.A. thanks the Ministerio de Ciencia y Tecnología for a doctoral fellowship.

[1] P. I. Dalko, L. Moisan, *Angew. Chem. Int. Ed.* **2001**, *40*, 3726.
[2] W. Notz, F. Tanaka, C. F. Barbas III, *Acc. Chem. Res.* **2004**, *37*, 580.
[3] D. B. Ramachary, N. S. Chowdari, C. F. Barbas III, *Tetrahedron Lett.* **2002**, *43*, 6743.
[4] B. List, *Tetrahedron* **2002**, *58*, 5573.
[5] a) Z. G. Hajos, D. R. Parrish, *J. Org. Chem.* **1974**, *39*, 1615; b) B. List, P. Pojarliev, C. Castello, *Org. Lett.* **2001**, *3*, 537; c) A. B. Northrup, D. W. C. MacMillan, *J. Am. Chem. Soc.* **2002**, *124*, 6798.
[6] a) A. Cordova, W. Notz, G. Zhong, J. M. Betancort, C. F. Barbas III, *J. Am. Chem. Soc.* **2002**, *124*, 1842; b) P. Pojarliev, W. T. Biller, H. J. Martin, B. List, *Synlett* **2003**, 1903; c) W. Notz, F. Tanaka, S. Watanabe, N. S. Chowdari, J. M. Turner, R. Thayumanavan, C. F. Barbas III, *J. Org. Chem.* **2003**, *68*, 9624.
[7] a) T. Bui, C. F. Barbas III, *Tetrahedron Lett.* **2000**, *41*, 6951; b) J. M. Betancort, K. Sakthivel, R. Thayumanavan, C. F. Barbas III, *Tetrahedron Lett.* **2001**, *42*, 4441; c) J. M. Betancort, K. Sakthivel, R. Thayumanavan, F. Tanaka, C. F. Barbas III, *Synthesis* **2004**, 1509.
[8] a) K. A. Ahrendt, C. J. Borths, D. W. C. MacMillan, *J. Am. Chem. Soc.* **2000**, *122*, 4243; b) R. Thayumanavan, B. Dhevalapally, K. Sakthivel, F. Tanaka, C. F. Barbas III, *Tetrahedron Lett.* **2002**, *43*, 3817.

[9] a) A. Kamimura, Y. Kaneko, A. Ohta, A. Kakehi, H. Matsuda, S. Kanemasa, *Tetrahedron Lett.* **1999**, *40*, 4349; b) A. Kamimura, Y. Kaneko, A. Ohta, K. Matsuura, Y. Fujimoto, A. Kakehi, S. Kanemasa, *Tetrahedron* **2002**, *58*, 9613; c) R. Zimmer, B. Orschel, S. Scherer, H.-U. Reißig, *Synthesis* **2002**, 1553; d) R. Zimmer, M. Hoffmann, H.-U. Reißig, *Chem. Ber.* **1992**, *125*, 2243; e) J. Angermann, K. Homann, H.-U. Reißig, R. Zimmer, *Synlett* **1995**, 1014; f) J. K. Gallos, V. C. Sarli, A. C. Varvogli, C. Z. Papadoyanni, S. D. Papaspyrou, N. G. Argyropoulos, *Tetrahedron Lett.* **2003**, *44*, 3905; g) S. Nakanishi, Y. Shirai, K. Takahashi, Y. Otsuji, *Chem. Lett.* **1981**, 869; h) R. Zimmer, H.-U. Reißig, *J. Org. Chem.* **1992**, *57*, 339; i) M. Buchholz, F. Hiller, H.-U. Reißig, *Eur. J. Org. Chem.* **2002**, 2838; j) C. Hippeli, H.-U. Reißig, *Liebigs Ann. Chem.* **1990**, 217; k) C. Hippeli, R. Zimmer, H.-U. Reißig, *Liebigs Ann. Chem.* **1990**, 469; l) P. Bravo, G. Gaudiano, P. P. Ponti, A. Umani-Ronchi, *Tetrahedron* **1970**, *26*, 1315; m) T. L. Gilchrist, G. M. Iskander, A. K. Yagoub, *J. Chem. Soc., Chem. Commun.* **1981**, 696; n) T. L. Gilchrist, G. M. Iskander, A. K. Yagoub, *J. Chem. Soc., Perkin Trans. 1* **1985**, 2769; o) C. Hippeli, H.-U. Reißig, *Liebigs Ann. Chem.* **1990**, 475.

[10] For a review of the asymmetric Diels–Alder reactions of nitroso compounds, see: Y. Yamamoto, H. Yamamoto, *Eur. J. Org. Chem.*, DOI:10.1002/ejoc.200500847.

[11] a) R. Faragher, T. L. Gilchrist, *J. Chem. Soc., Chem. Commun.* **1976**, 581; b) D. E. Davies, T. L. Gilchrist, T. G. Roberts, *J. Chem. Soc., Perkin Trans. 1* **1983**, 1275; c) T. L. Gilchrist, T. G. Roberts, *J. Chem. Soc., Perkin Trans. 1* **1983**, 1283; d) T. L. Gilchrist, *Chem. Soc. Rev.* **1983**, *12*, 53; e) R. Zimmer, H.-U. Reißig, *Angew. Chem. Int. Ed. Engl.* **1988**, *27*, 1518; f) H.-U. Reißig, C. Hippeli, T. Arnold, *Chem. Ber.* **1990**, *123*, 2403; g) K. Paulini, H.-U. Reißig, P. Rademacher, *J. Prakt. Chem.* **1995**, *337*, 209; h) D. Sperling, A. Mehlhorn, H.-U. Reißig, J. Fabian, *Liebigs Ann.* **1996**, 1615; i) R. Zimmer, J. Angermann, U. Hain, F. Hiller, H.-U. Reißig, *Synthesis* **1997**, 1467.

[12] J. Lee, L. Chen, A. H. West, G. B. Richter-Addo, *Chem. Rev.* **2002**, *102*, 1019.

[13] T. C. Wabnitz, S. Saaby, K. A. Jorgensen, *Org. Biomol. Chem.* **2004**, *2*, 828.

[14] a) L. R. Domingo, M. Arnó, M. J. Andrés, *J. Org. Chem.* **1999**, *64*, 5867; b) L. R. Domingo, A. Asensio, *J. Org. Chem.* **2000**, *65*, 1076; c) L. R. Domingo, A. Asensio, P. Arroyo, *J. Phys. Org. Chem.* **2002**, *15*, 660.

[15] S. E. Denmark, A. Thorarensen, *Chem. Rev.* **1996**, *96*, 137.

[16] R. G. Parr, L. von Szentpaly, S. Liu, *J. Am. Chem. Soc.* **1999**, *121*, 1922.

[17] P. Geerlings, F. De Proft, W. Langenaeker, *Chem. Rev.* **2003**, *103*, 1793.

[18] L. R. Domingo, M. J. Aurell, P. Pérez, R. Contreras, *Tetrahedron* **2002**, *58*, 4417.

[19] a) M. Arnó, L. R. Domingo, *Theor. Chem. Acc.* **2002**, *108*, 232; b) M. Arnó, L. R. Domingo, *Org. Biomol. Chem.* **2003**, *1*, 637; c) M. Arnó, R. J. Zaragozá, L. R. Domingo, *Tetrahedron: Asymmetry* **2004**, *15*, 1541; d) M. Arnó, R. J. Zaragozá, L. R. Domingo, *Tetrahedron: Asymmetry* **2005**, *16*, 2764.

[20] a) L. R. Domingo, *Tetrahedron* **2002**, *58*, 3765; b) L. R. Domingo, M. J. Aurell, *J. Org. Chem.* **2002**, *67*, 959; c) L. R. Domingo, M. J. Aurell, P. Pérez, R. Contreras, *J. Org. Chem.* **2003**, *68*, 3884; d) L. R. Domingo, J. Andrés, *J. Org. Chem.* **2003**, *68*, 8662; e) L. R. Domingo, *Eur. J. Org. Chem.* **2004**, 4788; f) P. Arroyo, M. T. Picher, L. R. Domingo, F. Terrier, *Tetrahedron* **2005**, *61*, 7359.

[21] W. L. Jorgensen, D. Lim, J. F. Blake, *J. Am. Chem. Soc.* **1993**, *115*, 2936.

[22] a) B. Jursic, Z. Zdravkovski, *J. Chem. Soc., Perkin Trans. 2* **1995**, 1223; b) B. Jursic, *J. Mol. Struc. (THEOCHEM)* **1996**, *365*, 55; c) E. Goldstein, B. Beno, K. N. Houk, *J. Am. Chem. Soc.* **1996**, *118*, 6036.

[23] W. J. Hehre, L. Radom, P. v. R. Schleyer, J. A. Pople, *Ab initio Molecular Orbital Theory*, Wiley, New York, **1986**.

[24] a) J. Cizek, *Adv. Chem. Phys.* **1969**, *14*, 35; b) G. D. Purvis, R. J. Bartlett, *J. Chem. Phys.* **1982**, *76*, 1910; c) E. Scuseria, C. L. Janssen, H. F. Schaefer III, *J. Chem. Phys.* **1988**, *89*, 7382; d) G. E. Scuseria, H. F. Schaefer III, *J. Chem. Phys.* **1989**, *90*, 3700.

[25] M. J. S. Dewar, S. Olivella, J. J. P. Stewart, *J. Am. Chem. Soc.* **1986**, *108*, 5771.

[26] L. R. Domingo, *J. Org. Chem.* **2001**, *66*, 3211.

[27] K. B. Wiberg, *Tetrahedron* **1968**, *24*, 1083.

[28] These calculations were performed following the suggestions of one referee.

[29] a) A. D. Becke, *J. Chem. Phys.* **1993**, *98*, 5648; b) C. Lee, W. Yang, R. G. Parr, *Phys. Rev. B* **1988**, *37*, 785.

[30] a) R. V. Stanton, K. M. Merz, *J. Chem. Phys.* **1994**, *100*, 434; b) J. E. Carpenter, C. P. Sosa, *J. Mol. Struct., (THEOCHEM)* **1994**, *311*, 325; c) J. Baker, M. Muir, J. Andzelm, *J. Chem. Phys.* **1995**, *102*, 2036; d) B. Jursic, Z. Zdravkovski, *J. Chem. Soc., Perkin Trans. 2* **1995**, 1223; e) E. Goldstein, B. Beno, K. N. Houk, *J. Am. Chem. Soc.* **1996**, *118*, 6036; f) V. Branchadell, J. Font, A. G. Moglioni, C. Ochoa de Echaguen, A. Oliva, R. M. Ortuño, J. Veciana, J. Vidal Gancedo, *J. Am. Chem. Soc.* **1997**, *119*, 9992; g) L. R. Domingo, M. Arnó, J. Andrés, *J. Am. Chem. Soc.* **1998**, *120*, 1617.

[31] a) H. B. Schlegel, *J. Comput. Chem.* **1982**, *3*, 214; b) H. B. Schlegel, "Geometry Optimization on Potential Energy Surface" in *Modern Electronic Structure Theory* (Ed.: D. R. Yarkony), World Scientific Publishing, Singapore, **1994**.

[32] K. Fukui, *J. Phys. Chem.* **1970**, *74*, 4161.

[33] a) C. González, H. B. Schlegel, *J. Phys. Chem.* **1990**, *94*, 5523; b) C. González, H. B. Schlegel, *J. Chem. Phys.* **1991**, *95*, 5853.

[34] a) A. E. Reed, R. B. Weinstock, F. Weinhold, *J. Chem. Phys.* **1985**, *83*, 735; b) A. E. Reed, L. A. Curtiss, F. Weinhold, *Chem. Rev.* **1988**, *88*, 899.

[35] M. J. Frisch, G. W. Trucks, H. B. Schlegel, G. E. Scuseria, M. A. Robb, J. R. Cheeseman, V. G. Zakrzewski, J. A. Montgomery, R. E. Stratmann, J. C. Burant, S. Dapprich, J. M. Millam, A. D. Daniels, K. N. Kudin, M. C. Strain, O. Farkas, J. Tomasi, V. Barone, M. Cossi, R. Cammi, B. Mennucci, C. Pomelli, C. Adamo, S. Clifford, J. Ochterski, G. A. Petersson, P. Y. Ayala, Q. Cui, K. Morokuma, D. K. Malick, A. D. Rabuck, K. Raghavachari, J. B. Foresman, J. Cioslowski, J. V. Ortiz, B. B. Stefanov, G. Liu, A. Liashenko, P. Piskorz, I. Komaromi, R. Gomperts, R. L. Martin, D. J. Fox, T. Keith, M. A. Al-Laham, C. Y. Peng, A. Nanayakkara, M. Challacombe, P. M. W. Gill, B. Johnson, W. Chen, M. W. Wong, J. L. Andres, C. Gonzalez, M. Head-Gordon, E. S. Replogle, J. A. Pople, Gaussian 98, Revision A.6, Gaussian, Inc., Pittsburgh PA, **1998**.

[36] a) J. Tomasi, M. Persico, *Chem. Rev.* **1994**, *94*, 2027; b) B. Y. Simkin, I. Sheikhet, *Quantum Chemical and Statistical Theory of Solutions-A Computational Approach*, Ellis Horwood, London, **1995**.

[37] a) E. Cances, B. Mennucci, J. Tomasi, *J. Chem. Phys.* **1997**, *107*, 3032; b) M. Cossi, V. Barone, R. Cammi, J. Tomasi, *Chem. Phys. Lett.* **1996**, *255*, 327; c) V. Barone, M. Cossi, J. Tomasi, *J. Comput. Chem.* **1998**, *19*, 404.

[38] a) R. G. Parr, R. G. Pearson, *J. Am. Chem. Soc.* **1983**, *105*, 7512; b) R. G. Parr, W. Yang, *Density Functional Theory of Atoms and Molecules*, Oxford University Press, New York, **1989**.

[39] a) R. F. W. Bader, *Acc. Chem. Res.* **1985**, *18*, 9; b) R. F. W. Bader, *Atoms in Molecules: A Quantum Theory*, Oxford University Press, Oxford, **1990**.

[40] A. D. Becke, K. E. Edgecombe, *J. Chem. Phys.* **1990**, *92*, 5397.

[41] a) A. Savin, A. D. Becke, J. Flad, R. Nesper, H. Preuss, H. G. von Schnering, *Angew. Chem. Int. Ed. Engl.* **1991**, *30*, 409; b) B. Silvi, A. Savin, *Nature* **1994**, *371*, 683.

[42] a) M. D. Michelini, E. Sicilia, N. Russo, M. E. Alikhani, B. Silvi, *J. Phys. Chem. A* **2003**, *107*, 4862; b) E. Chamorro, R. Notario, *J. Phys. Chem. A* **2004**, *108*, 4099; c) S. Berski, J. Andres, B. Silvi, L. R. Domingo, *J. Phys. Chem. A* **2003**, *107*,

6014; d) V. Polo, J. Andres, R. Castillo, S. Berski, B. Silvi, *Chem. Eur. J.* **2004**, *10*, 5165; e) J. C. Santos, J. Andres, A. Aizman, P. Fuentealba, V. Polo, *J. Phys. Chem. A* **2005**, *109*, 3687; f) C. Cárdenas, E. Chamorro, R. Notario, *J. Phys. Chem. A* **2005**, *109*, 4352; g) J. C. Santos, V. Polo, J. Andres, *Chem. Phys. Lett.* **2005**, *406*, 393; h) M. D. Michelini, N. Russo, M. E. Alikhani, B. Silvi, *J. Comput. Chem.* **2005**, *26*, 1284; i) V. Polo, J. Andres, *J. Comput. Chem.* **2005**, *26*, 1427; j) E. Chamorro, *J. Chem. Phys.* **2005**, *118*, 8687.

[43] S. Noury, X. Krokidis, F. Fuster, B. Silvi, *Comput. Chem.* **1999**, *23*, 597.

Received: December 15, 2005
Published Online: March 27, 2006

